Energy, Mines and Resources Canada | Énergie, Mines et Ressources Canada

CANMET

Canada Centre for Mineral and Energy Technology | Centre canadien de la technologie des minéraux et de l'énergie

WELDING PROCEDURES FOR THE FABRICATION OF THICK SECTION 2.25Cr-1Mo PRESSURE VESSEL STEEL

J.T. MCGRATH, J.A. GIANETTO and R.F. ORR
WELDING SECTION

JANUARY 1987

PHYSICAL METALLURGY RESEARCH LABORATORIES

28 pp
REPORT: ~~PMRL~~ PNRL 87-12(TR)

PHYSICAL METALLURGY RESEARCH LABORATORIES

REPORT: PMRL 87-12(TR)

WELDING PROCEDURES FOR THE FABRICATION OF THICK SECTION 2.25Cr-1Mo PRESSURE VESSEL STEEL

by

J.T. McGrath, J. .A. Gianetto and R.F. Orr

ABSTRACT

Welding procedures were investigated to join 2.25Cr -1Mo steel using the submerged-arc narrow-gap (SAW-NG) process. Welding consumables (Oerlikon EB-3 wire and OP76 flux) were chosen which resulted in a fine, bainitic microstructure and low inclusion content ($O+S \leq 0.035\%$) for welds deposited within the energy input range of 2-4 kJ/mm. Employing this procedure, a thick-section (150 mm) 2.25Cr-1Mo steel weldment was prepared using the SAW-NG process. The resultant weld exceeded the strength and notch toughness property requirements.

LABORATOIRES DE RECHERCHE EN METALLURGIE PHYSIQUE

RAPPORT: PMRL 87-12(TR)

PROCEDES DE SOUDAGE POUR RECIPIENTS SOUS PRESSION A PAROI EPAISSE EN ACIER 2.25Cr-1Mo

par

J.T.McGrath, J.A. Gianetto et R.F. Orr

RESUME

On a étudié des méthodes de soudage permettant d'assembler des aciers 2.25Cr-1Mo à l'aide du procédé de soudage à l'arc sous flux électroconducteur à écartement étroit. Dans le cadre de cette étude, on a choisi des produits auxiliaires de soudage de la composition suivante (fil Oerlikon EB-3 et flux OP76). Ces produits ont donné une microstructure bainitique fine avec un faible taux d'inclusions ($O + S \leq 0{,}035\%$) pour les soudures réalisées dans la gamme d'apport de chaleur de 2-4 kJ/mm. A l'aide de cette méthode, une soudure d'une plaque d'acier épaisse (150 mm) contenant 2.25Cr-1Mo a été préparée avec le procédé de soudage a l'arc sous flux à écartement étroit. Les résultats obtenus avec cette soudure dépassaient les exigences au niveau de la force et de la résistance à l'entaille.

INTRODUCTION

Considerable research work has been done on the evaluation of the submerged-arc narrow-gap (SAW-NG) weldments designed for use in the fabrication of reactor vessels within the petro-chemical industry. In particular, the microstructure/mechanical property relationships of 2.25Cr-1Mo (1-3) and C-Mn, A516-Gr 70 (4) steel weldments, using commercially available consumables, have been studied in intermediate thickness materials (40-75 mm)

Based on these preliminary studies and because of the stringent requirements placed on thick section 2.25Cr-1Mo steel weldments further study was necessary to establish the appropriate welding conditions and weld metal chemistry in order to achieve the following mechanical properties in thick section (≥150 mm) weld metals.

Yield Strength	420 MPa (min)
Tensile Strength	515-790 MPa
Charpy Impact Energy	54J @ -40°C PWHT

In the present study the main objectives were to (a) finalize the optimum weld procedure and weld chemistry for 2.25Cr-1Mo weld deposits, and (b) to use this procedure to prepare an SAW-NG weld in a thick-section (150 mm) 2.25Cr-1Mo steel plate that would meet the mechanical property requirements.

OPTIMIZATION OF WELD PROCEDURES AND WELD CHEMISTRY

Preparation of SAW-NG Welds

A series of narrow-gap welds (SAW-NG)were prepared in the 2.25Cr-1Mo steel. The work was done to formulate an optimum welding procedure and weld chemistry for the welding of a thick- section narrow-gap weldment. In this preliminary work, the influence of weld chemistry and energy input (cooling rate) on microstructure and mechanical properties was evaluated.

The series A welds were deposited in 38 mm thick plate using a range of currently available submerged-arc welding (SAW) consumables (Table 1). Some of the series A weld data has been reported previously (1). An AC square wave power source was used to prepare the welds with the parameters given in Table 2. A two-pass per layer welding technique was employed to join a near parallel-sided weld preparation (4° included angle) with a 15 mm root gap (Fig. 1).

Additionally, in the series B experiments, welds were prepared in order to provide a better understanding of the influence of energy input (cooling rate) and weld chemistry on the as-deposited microstructure of 2.25Cr-1Mo SAW. The experiment consisted of a series of bead-on-plate (BOP), undiluted test pads, deposited using the Oerlikon-Armco W22 wire with an acid (Linde 124) and basic (OP76) flux.. The BOP welds were made using an AC square wave power source and a range of energy inputs, i.e., 2, 4 and 6 kJ/mm. The welding parameters are listed in Table 3.

All welds were subjected to a post-weld heat treatment (PWHT) of 690°C for 10 hours. The tensile strength of the series A welds was measured from all

weld metal tensile specimens and the Charpy impact energy was determined as a function of temperature for specimens notched through-thickness with the notch positioned in the centre of the weld beads at the 1/4W position (where W = weld width).

The weld metal microstructures were characterized using the light microscope supported by selected electron microscopy. In addition, carbide precipitation was characterized for the series B welds W7 and W9 deposited at energy inputs of 2 and 6 kJ/mm. Two stage carbon replicas were taken from the as-deposited region of both samples. The replicas were examined in a Philips 400 TEM/STEM microscope.

RESULTS

Weld Chemistry

The chemical compositions of the SAW-NG welds from series A are listed in Table 4. The weld compositions were dependent upon wire composition and flux basicity. The dilution from the base metal was approximately 10 per cent. The compositional difference with respect to carbon, manganese, silicon and oxygen can be related primarily to flux basicity. The acid (B.I.= 1) Linde 124 flux resulted in lower carbon and higher manganese, silicon and oxygen levels in welds W2 and W4 compared with the other welds deposited with the basic fluxes. The higher sulphur levels observed in welds W4, W5 and W6 were attributed to the wire composition.

The compositions of the series B welds which were made with varying energy input and flux basicity are presented in Table 5. The only compositional change which could be attributed to increasing energy input was the reduction

in oxygen content. The differences in carbon, manganese, silicon and oxygen contents when comparing welds W7, W8 and W9 with W10, W11 and W12 can be explained, as before, on the basis of flux basicity.

Weld Metal Microstructure

The macrostructure of the 2.25Cr-1Mo narrow-gap welds was composed of as-deposited and reheated regions in which the as-deposited region was subjected to the thermal effects of subsequent passes. Figure 2 shows a typical distribution of these regions. Within both the as-deposited and reheated regions a totally bainitic transformation structure was formed.

Using the terminology of Torronen (5) and Kotilainen (6), the bainitic structure within a prior austenite grain was composed of individual bainitic packets which formed bundles. The packets in the welds were elongated in shape and approximately 3 to 6 μm wide. These packets are the smallest units surrounded by high-angle boundaries. The packets are further sub-divided into parallel laths, where the misorientation across lath boundaries, as determined by TEM, was of the order of 1 to 2 degrees.

Representative micrographs of the SAW-NG, Series A welds are shown in Fig. 3. The packet characteristics, i.e., width and shape, varied for welds W1 to W6. In welds W1 and W3 the packets were elongated or plate-like whereas the packets in welds W2, W4, in particular, were wider and more irregular in shape.

The effects of varying energy input (cooling rate) and flux basicity on weld microstructure are shown in Fig.4. Welds deposited with basic flux exhibited fine, plate-like bainitic packets for both the 2 and 4 kJ/mm energy inputs. There was only a slight increase in packet dimensions at the highest energy

input of 6 kJ/mm. Similarily the microstrucutres of the welds W10, W11 and W12, deposited with the acid flux, were not greatly affected by increasing energy input. However, the differences in chemical composition, particularly the lower carbon, resulted in the packets being coarser and more irregular in shape Fig. 4 (c) and (d) compared with the corresponding welds made with the basic flux.

Carbide and Inclusion Formulation

In the present study, weld W7 contained globular shaped precipitates of the order of 0.1 μm to 0.4 μm; some rod-shaped precipitates 0.4 μm to 0.6 μm in length and some fine needle-shaped precipitates 0.1 μm to 0.2 μm in length (Fig. 5(a)). Both the globular and rod-shaped precipitates were chromium- and iron-rich and are probably the more stable M_7C_3, $M_{23}C_6$ and M_6C carbides identified by Lundin et al (7) and Swift and Rogers(8). These precipitates were found along grain boundaries and within the matrix. The needle-shaped particles (likely M_2C) were molybdenum-rich and were located within the matrix. Weld W9 (Fig. 5(b)) displayed fewer globular-shaped precipitates and more rod-shaped and needle-shaped precipitates than weld W7. The precipitates were slightly larger for weld W9 but the composition of the precipitates and their location were similar to that of weld W7.

The inclusion particles in all welds were spherical in shape as observed in optical microscopy examination. Although no identification of their composition was attempted, it was assumed that they were mainly oxysulphides. The volume fraction of inclusions is directly proportional to the oxygen and sulphur contents of the weld metals. For both the series A and series B weldments the highest inclusion contents were produced in those welds deposited with the acid flux.

Mechanical Properties

The mechanical property data for welds W1 to W6 are presented in Table 6. All welds exceeded the minimum yield strength requirement of 420 MPa, with weld W1 achieving the highest strength. Only welds W1 and W3 met the low temperature impact requirement of 54 J at -40°C. In terms of the resistance to ductile fracture, welds W1 and W3 also exhibited the highest impact energies at 25°C. Generally there was a trend towards decreasing impact energy at 25°C with increasing O+S content.

DISCUSSION

The results have indicated that the shape and size of the bainitic packets in the fully bainitic weld metal microstructure were dependent primarily on the transformation temperature which is dictated by the weld composition, in particular, the carbon content. The empirical equation (9) for the bainite start transformation temperature, B_S = 830 - 270C - 90Mn - 37Ni - 70Cr - 83Mo indicates that carbon has the most significant effect on the bainite transformation temperature.

The observations also indicated that a fine bainite packet size was associated with welds with a low inclusion content and a coarse packet size with a high inclusion content. Therefore, an argument might be put forward that the oxygen content in the form of weld metal inclusions played a role in controlling the bainite packet size as it does for acicular ferrite nucleation in low alloy weld metals (10). The definitive work by Ito et al (11) and Chandel et al (3) on SAW 2.25Cr-1Mo weld metals has shown, however, that for welds with a low inclu-

sion content (O+S≤0.040) increasing the carbon level in the range of 0.06 to 0.11% was the most significant factor in refining the bainitic packet size.

The further observation that the bainitic packet size did not change significantly with energy input (cooling rate) can be explained from the CCT diagram of 2.25Cr-1Mo in Fig. 6 (12). Figure 6 indicates that for a given composition the bainitic region extends over a wide range of cooling rates and that the transformation temperature does not vary appreciably over this range. The work of Torronen (5) which was performed on a continuously cooled 2.8Cr-0.6Mo-0.3V alloy also indicated that the dimensions of the bainite packets were dependent upon the transformation temperature and were independent of the prior austenitizing temperature and cooling rate.

The resultant notch toughness properties can be explained in terms of the weld microstructural characteristics. The low temperature resistance to cleavage fracture can be related to bainite packet size. The work of Kotilainen (6) has shown that the grain size unit that controls the resistance to cleavage fracture in a continuously cooled and tempered bainitic Cr-Mo-V steel is the bainitic packet size. The unit fracture length corresponded with the bainite packet width, suggesting that the finer the packet size, the higher the resistance to cleavage fracture. Examination of fractured surfaces by Kotilainen revealed that the average cleavage facet size corresponded very well with the width of the bainitic packets. For the current results, the fine bainitic structure of welds W1 and W3 resulted in excellent low temperature notch toughness compared with the coarser bainite of welds W2 and W4. Fractographic evidence and the work of Kotilainen (6) also indicated that the cleavage facets and bainitic packets had similar dimensions, i.e., the width was of the order of 3 to 6 μm. The fracture mechanism probably involves cleavage initiation and propagation

across a bainite packet, with re-initiation taking place at each high-angled packet boundary.

The resistance to ductile fracture in 2.25Cr-1Mo weld metal was found to be related to inclusion volume fraction represented by the O+S content of the weld. As shown in Table 6, the Charpy impact energy at 25°C decreased as the O+S increased. Both welds W3 and the thick section weld CRM-1, with the lowest level of O+S, had the highest impact energy at 25°C. The spherical oxy-sulfide inclusion particles act as sites for microvoid coalescence when the fracture mode is by ductile tearing. It should be noted that the effect of inclusions is not only to lower the Charpy upper shelf region but also to shift the Charpy curve to higher temperatures. This is the reason that welds W5 and W6, which had a relatively fine bainitic microstrucutre by virture of the optimum level of 0.1% carbon, exhibited poor fracture resistance at -40°C. The higher sulphur levels (0.016%) in these welds contributed to the higher oxysulfide inclusion content and the resultant shift in the Charpy transition curve to higher temperatures.

Finally, the observations of carbide morphology and composition relate principally to their effect on creep strength of 2.25Cr-1Mo weld metals. The work of Lundin (7) has indicated that the fine, needle-like M_2C carbides are more effective in providing creep strength than the coarser, spheriordized $M_{23}C_6$, M_7C_3 and M_6C carbides. The M_2C carbides form at lower tempering temperatures and times represented by the tempering parameter equation, $TP = T(20+\log t)x10^{-3}$ while the coarser, spheriodized carbides predominate at higher tempering temperatures and times. In summary, these experiments on narrow-gap welding of 2.25Cr-1Mo steel have shown that the most essential elements in the weld chemistry for controlling the weld microstructure and the re-

sultant mechanical properties are carbon, sulphur and oxygen. In order to achieve the optimum levels of carbon (0.1%) and oxygen + sulphur (≤0.035%) in the weld deposit the Oerlikon-Armco W22 wire with C = 0.12% and S <0.01% and a highly basic flux (OP76) are recommended. There is some flexibility in the selection of the welding operating parameters, i.e. energy input. It was shown that a fine bainitic weld microstructure could be obtained over the energy input range of 2 - 4 kJ/mm

PREPARATION AND EVALUATION OF A THICK SECTION NARROW-GAP WELD

Utilizing the optimum weld procedure and weld chemistry data from the initial experiments on the series A and series B welds di-pass narrow-gap weld was prepared in a thick section, (150 mm), 2.25Cr-1Mo steel. The weld preparation and electrode placement are indicated in Fig. 1. An energy input of 2kJ/mm, with the welding parameters listed in Table 7, was used to deposit the weld. The welding consumables were the Oerlikon-Armco W22 wire (3.2 mm diam) and OP76 flux. The compositions of the base plate and wire are included in Table 8.

Weld Structure and Mechanical Properties

The weld metal chemistry is shown in Table 8. The carbon level of 0.09% is just slightly below the optimum level of 0.1%, while the S+O at 0.024% is well below the recommended level of ≤ 0.035%. The macrosection in Fig. 7 indicates bead shape and overlap in the narrow-gap weld. The fine, plate-like bainitic microstructure in Fig. 8 was comparable to the microstructure of weld W3 (Fig. 3(a)) which resulted in the highest low temperature weld metal tough-

ness properties in the series A experiments.

The mechanical properties of the heavy section narrow-gap weld are summarized in Table 9. The yield and ultimate tensile strengths are within the required levels of 420 MPa minimum, and the range 515-690 MPa, respectively. The Charpy impact energies at -40°C and 25°C were very high, exceeding, in particular, the 54 J requirement at -40°C.

CONCLUSIONS

1. The notch toughness requirement of 54 J at -40°C was achieved in 2.25Cr-1Mo narrow-gap submerged-arc weld deposits containing a fine bainitic microstructure combined with a low inclusion content (O+S ≤ 0.035%).

2. The weld microstructure was significantly influenced by the carbon level in the weld deposit. A level of 0.1% C resulted in a fine grained bainitic microstructure.

3. The optimum levels of carbon (0.1%) and oxygen + sulphur (≤0.035%) in the weld deposit were achieved using th Oerlikon-Armco W22 wire with C = 0.12% and S < 0.01% combined with the highly basic Oerlikon OP76 flux.

4. A fine bainitic weld microstructure was obtained over an energy input range of 2 - 4 kJ/mm using the basic OP76 flux.

5. Employing an Oerlikon-Armco W22 wire and OP76 flux and an energy input of 2kJ/mm a narrow-gap submerged-arc weld was deposited in a thick section, 150 mm plate of 2.25Cr-1Mo steel. This weld exceeded the strength and notch toughness property requirements.

ACKNOWLEDGEMENTS

The authors would like to thank Mr. D. Dolan for preparation of the narrow-gap welds and Miss. J. Ng Yelim for the characterization of the weld precipitates by electron microscopy.

REFERENCES

1. Chandel, R.S., Orr, R.F., Gianetto, J.A., McGrath, J.T. and Knight, R.F., Mechanical Properties of 2.25 Cr -1 Mo Welds Deposited by SAW-NG Process, J. of Met. for Energy Systems, 7, (2) pp. 137-146 (1985).
2. Chandel, R.S. Orr, R.F., Gianetto, J.A., McGrath, J.T., Patchett,, B.M. and Bicknell, A.C. The Microstructure and Mechanical Properties of Narrow-Gap Welds in 2.25 Cr - 1 Mo Steel, Int. Ist. of Welding Doc: IX-1355-85, 1985.
3. Chandel, R.S., Orr, R.F., Gianetto, J.A., McGrath, J.T., and Wright, B., Some Factors Affecting The Mechanical Properties of Submerged-Arc Narrow-Gap Welds, Proc. Int. Conf. Welding for Challenging Environments, Pergamon Press, Toronto, pp 97-109, (1985).
4. McGrath, J.T. Chandel, R.S., Orr, R.F., Gianetto, J.A., Microstrucutre/Mechanical Property Relationships in Thick Section C-Mn Narrow-Gap Welds, submitted for publication to Welding Journal, 1987.
5. Torronen, K., Microstructural Parameters and Yielding in Quenched and Tempered Cr-Mo-V Pressure Vessel Steel, Tech. Research Centre of Finland, Publ. 22, (1979).
6. Kotilainen, H., The Micromechanisms of Cleavage Fracture and their Relationship to Fracture Toughness in a Bainitic low alloy steel, Tech Research Centre of Finland, Publ. 23, (1980).
7. Lundin, C.D., Kelley, S.C., Menon, R. and Kruse, B.J., Stress Rupture Behaviour of PWHT 2.25Cr-1Mo Weld Metal, Welding Research and

Engineering Group, Materials Science and Engineering Dept., University of Tennessee, Report, Jan., (1986).

8. Swift, R.A. and Rogers, H.C., Embrittlement of 2.25Cr-1Mo Steel Weld Metal by Postweld Heat Treatment, Welding J., 52 (4), Res. Suppl., p. 145s - 153s, (1973).

9. Pickering, F.B., High-strength, Low Alloy Steels - A Decade of Progress, Proc. Conf., Microalloying 75, Union Carbide Corp., pp. 9-55, (1975).

10. Cochrane, R.C. and Kirkwood, P.R., The Effect of Oxygen on Weld Metal Microstrucutre, Int. Conf., Trends in Steels and Consumables for Welding, The Welding Institute , Vol. 1, pp. 103-121, (1978).

11. Ito, Y., Nakanishi, M, Katsumoto, N and Tsumura, H., Improvement of Toughness and Reduction of Temper Embrittlement in 2.25 Cr-1 Mo Weld Metal, The Sumitomo Search, No 30, pp. 41-52, (1985).

12. Wada, T. and Eldis, G.T., Transformation Characteristics of 2.25 Cr-1 Mo Steel, ASTM STP 755, ASTM, pp.343-362, (1982).

Table 1. Submerged - arc welding consumables for series A welds

Weld no.	Consumables	
	Wire	Flux
W1	Oerlikon OE-SD2 CrMo (AWS EB3)	OP121TT
W2		Linde 124
W3		OP76
W4	Linde U 521 (AWS EB3)	Linde 124
W5		OP121TT
W6		OP76

Flux Basicity Index (B.I.) - OP121TT = 3.0
OP76 = 2.7
Linde 124 = 1.0

Table 2. Typical welding parameters for submerged - arc narrow - gap welds of series A

Current AC Square Wave (A)	Voltage (V)	Travel Speed (mm/s)	Electrical Stickout (mm)	Wire Size (mm)
450 - 500	30 - 34	6.7 -8.3	32	3.2

Preheat Temperature = 200°C

Interpass Temperature = 250 °C (max)

Table 3. Welding parameters for series B BOP welds

Heat input (kJ/mm)	Current AC square wave (A)	Voltage (V)	Travel speed (mm/s)	Electrical stickout (mm)
2	550	32	8.5	32
4	550	32	4.2	32
6	550	32	2.8	32

Maximum interpass temperature = 250°C

Table 4. Chemical composition of submerged - arc series A narrow - gap welds

Weld No.	Element Wt %										
	C	Mn	Si	S	P	Cr	Mo	Ni	Cu	Sn	O
W1	0.10	0.55	0.22	0.009	0.013	2.68	1.05	0.21	0.40	0.001	0.026
W2	0.06	0.67	0.49	0.011	0.009	2.63	1.06	0.21	0.38	< 0.005	0.085
W3	0.10	0.53	0.19	0.007	0.007	2.70	1.03	0.20	0.40	< 0.005	0.022
W4	0.06	0.66	0.43	0.022	0.008	2.24	1.06	0.09	0.33	< 0.005	0.077
W5	0.10	0.54	0.17	0.016	0.010	2.32	0.98	0.08	0.30	< 0.005	0.033
W6	0.10	0.54	0.16	0.016	0.007	2.32	1.00	0.09	0.30	< 0.005	0.027
SD-2 Wire	0.12	0.48	0.14	0.007	0.007	2.83	0.82	-	0.34	0.020	-
U-521 Wire	0.10	0.59	0.20	0.019	0.007	2.36	0.78	-	0.24	0.030	-
Base Plate	0.10	0.49	0.20	0.028	0.008	2.27	1.03	0.33	0.24	0.005	-

Table 5. Chemical composition of submerged - arc bead-on-plate series B welds deposited at a range of heat input

Weld No *	Energy Input * kJ/mm	Element wt %											
		C	Mn	Si	S	P	Cr	Mo	Ni	Cu	Sn	N	O
W7	2	0.11	0.56	0.15	0.006	0.008	2.71	1.04	0.19	0.36	0.005	0.0103	0.0216
W8	4	0.10	0.59	0.16	0.005	0.009	2.75	1.01	0.19	0.42	0.005	0.0107	0.0165
W9	6	0.11	0.60	0.19	0.005	0.009	2.75	1.01	0.19	0.39	0.005	0.0109	0.0172
W10	2	0.06	0.63	0.39	0.007	0.007	2.47	0.97	0.20	0.33	0.005	0.0105	0.0835
W11	4	0.06	0.63	0.38	0.007	0.008	2.45	0.98	0.20	0.40	0.005	0.0105	0.0715
W12	6	0.06	0.63	0.38	0.007	0.008	2.45	0.98	0.20	0.40	0.005	0.0099	0.0616

* Welds W7, W8, W9 and W10, W11, W12 were made using OP76 and Linde 124 fluxes, respectively.

Table 6 Mechanical properties of series A welds

Weld No.	YS MPa	UTS MPa	Impact -40°C	Energy,J 25°C	O+S wt%
W1	492	610	73	213	0.035
W2	468	592	20	98	0.096
W3	455	595	140	258	0.029
W4	436	565	8	62	0.099
W5	476	588	16	142	0.049
W6	450	575	18	172	0.043

Table 7 Welding parameters for a thick-section submerged-arc narrow-gap weld

Current AC Square Wave (A)	Voltage (V)	Travel Speed (mm/s)	Electrical Stickout (mm)	Wire Size (mm)
480-500	32	6.6-7.6	32	3.2

Table 8. Chemical compositions of thick-section submerged arc narrow gap weld, base plate, and welding wire.

Material	C	Mn	Si	S	P	Cr	Mo	Ni	Cu	Sn	N	O
CRM-1 Weld	0.09	0.55	0.19	0.005	0.006	2.76	0.99	0.19	0.32	0.005	0.014	0.019
Base Plate	0.16	0.54	0.14	0.002	0.003	2.45	0.98	0.02	-	0.002	-	-
OERLIKON -ARMCO W22(EB-3) wire	0.12	0.53	0.15	0.009	0.010	2.76	1.00	-	0.22	-	-	-

Table 9. Mechanical properties of thick section narrow gap weld.

Weld No.	YS MPa	UTS MPa	Impact Energy, J -40°C	25°C	O+S wt %
CRM-1	433	562	152	exceeded 300J	0.024

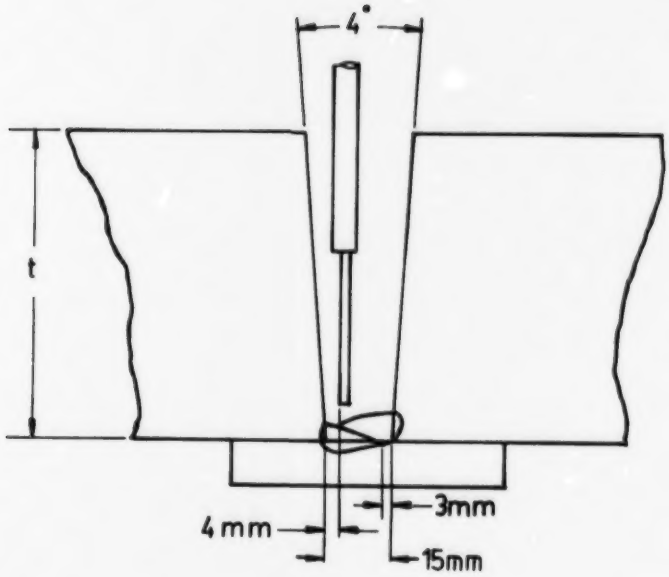

Fig. 1. Weld preparation and electrode placement for SAW-NG welds. (neg 15122)

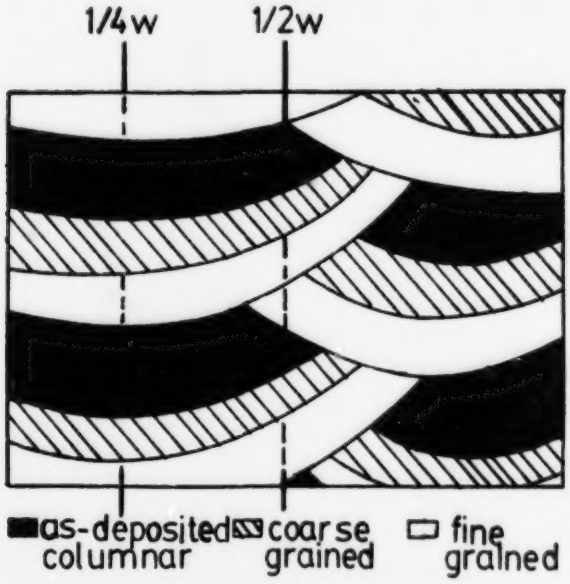

Fig. 2. Schematic representation of as-deposited and reheated weld metal regions. (neg 15121)

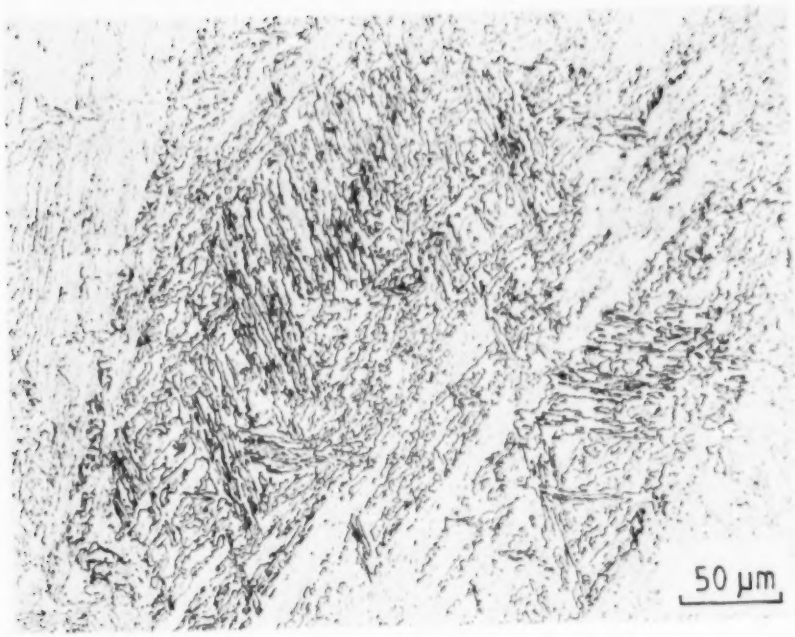

(a) weld W3 (neg 13367)

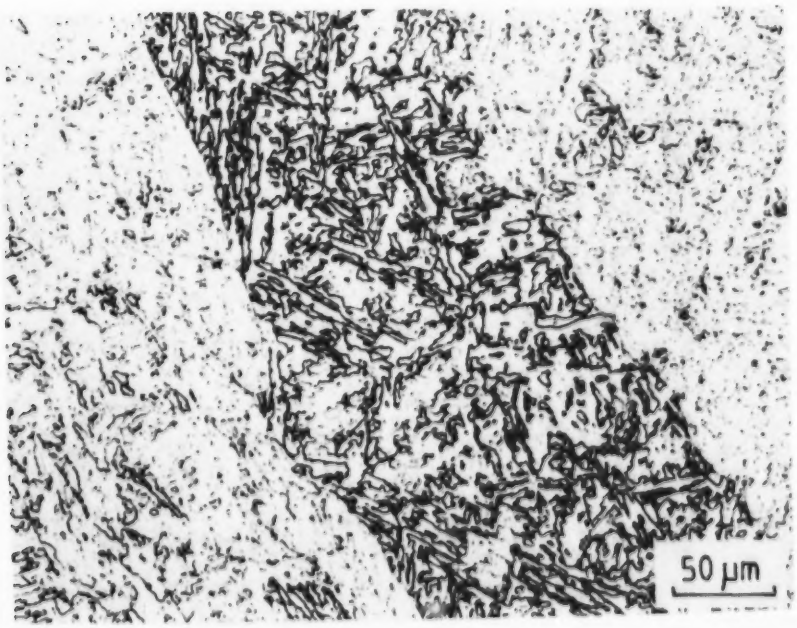

(b) weld W2 (neg 12265)

Fig. 3. Microstructures of series A SAW

Basic

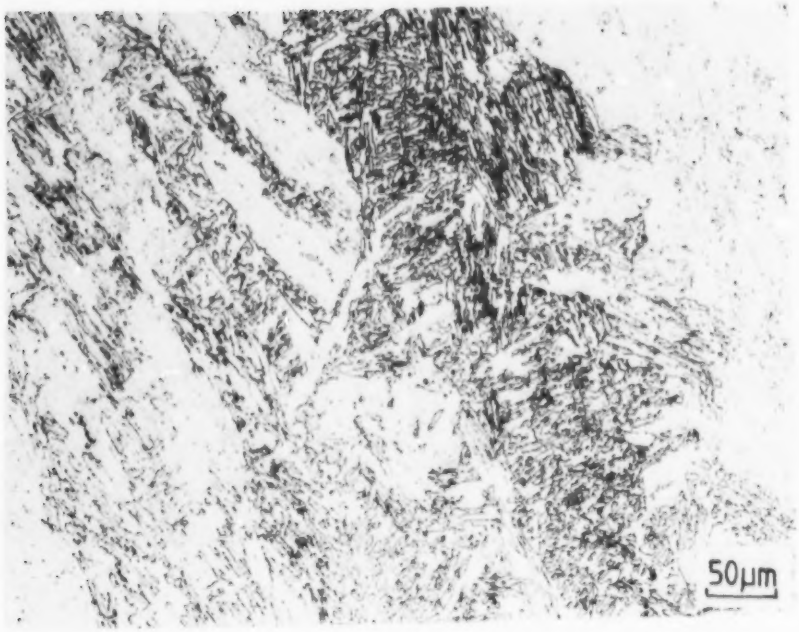

(a) 4kJ/mm (neg 15167)

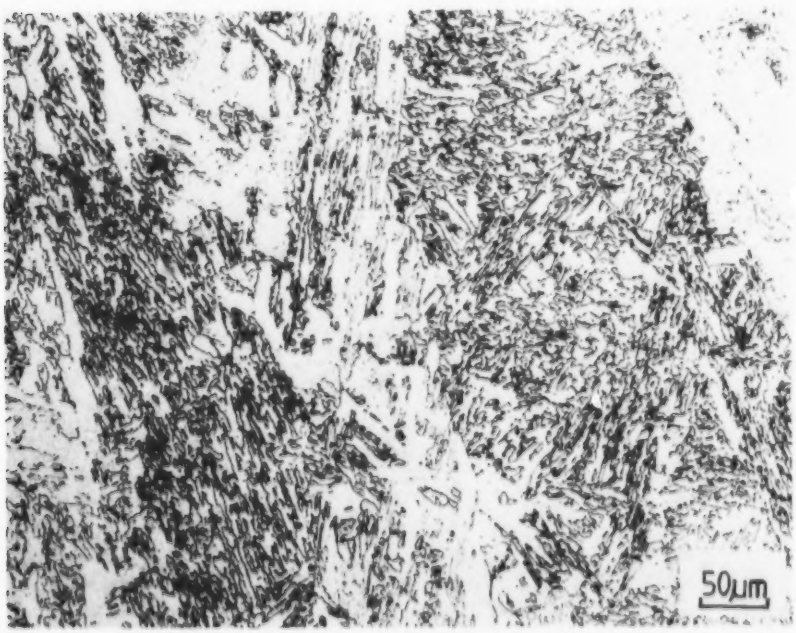

(b) 6kJ/mm (neg 14582)

Fig. 4 cont'd.

Acid

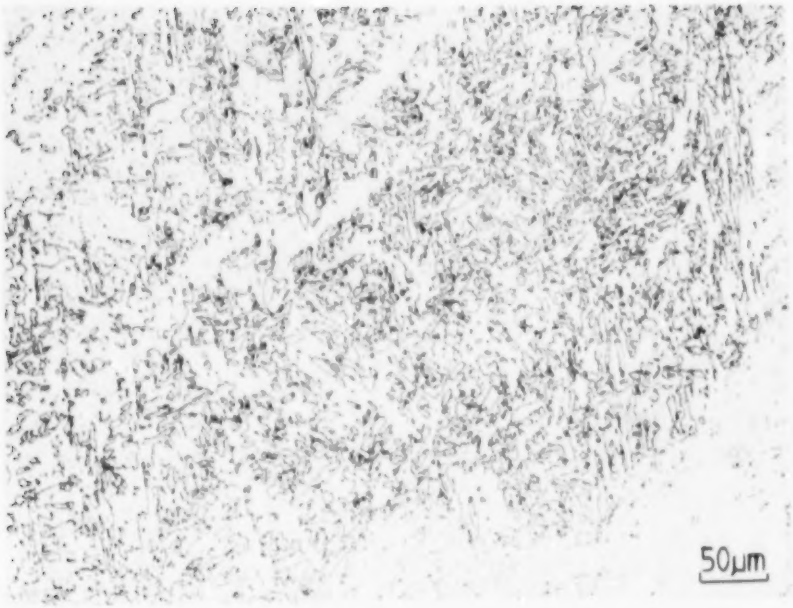

(c) 4 kJ/mm (neg 15361)

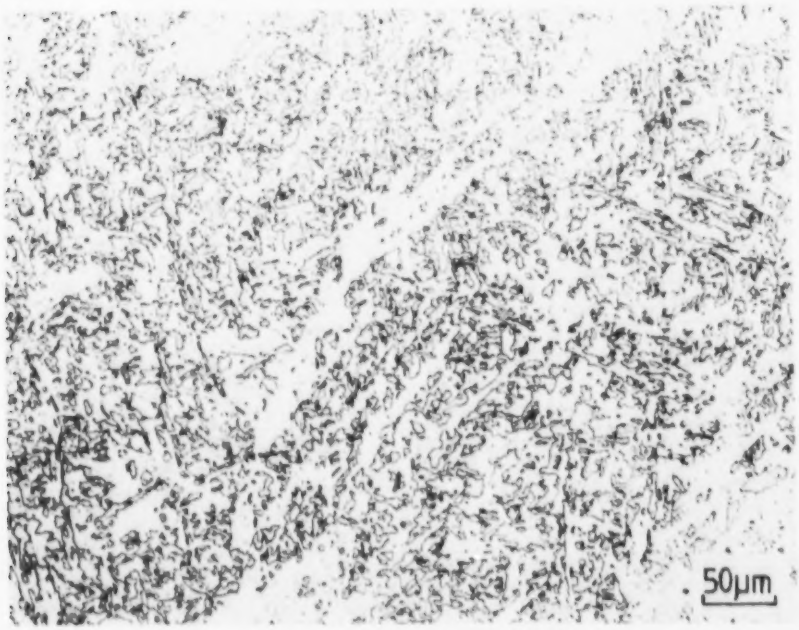

(d) 6kJ/mm (neg 15368)

Fig. 4. Microstructures of series B welds deposited at 4 and 6 kJ/mm using a basic and an acid flux.

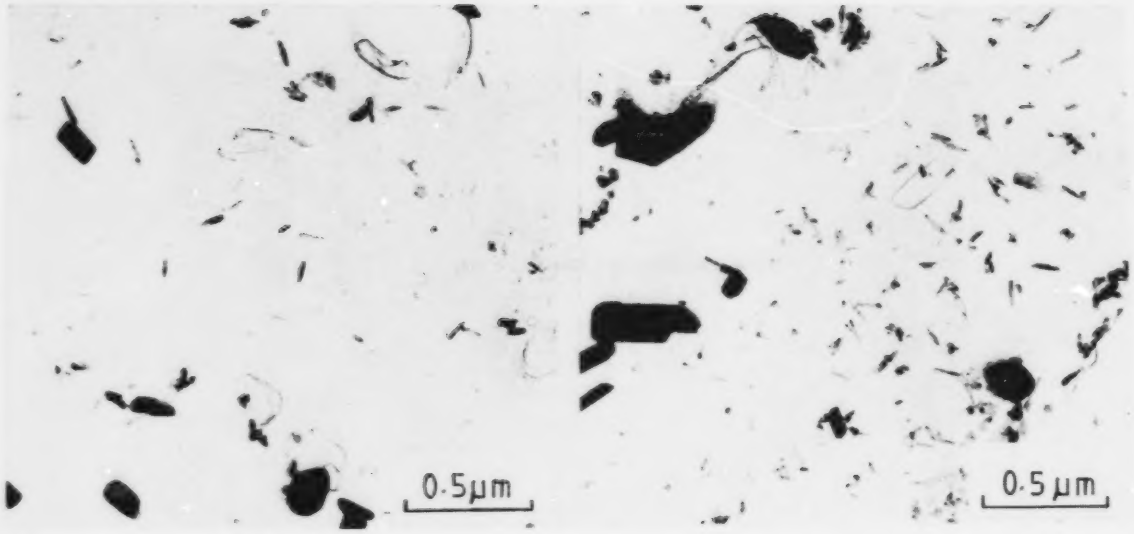

(a) weld W7 (b) weld W9

Fig. 5. TEM micrograph of carbide precipitates for welds deposited at 2 and 6 kJ/mm using a basic flux.

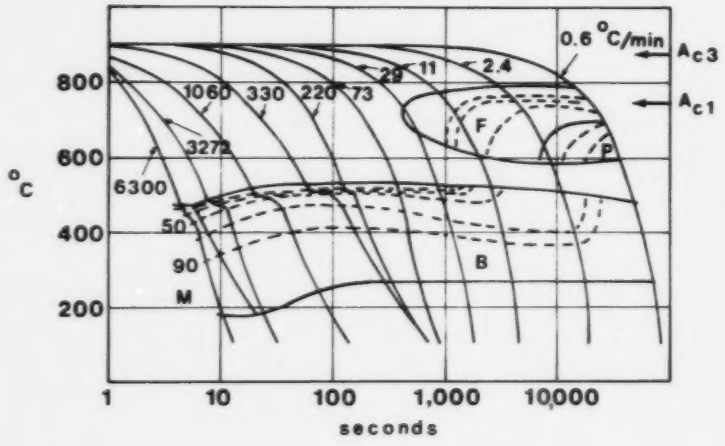

Fig. 6. CCT diagram of 2.25 Cr-1Mo steel (neg 14479)

C	Si	Mn	Cr	Mo
0.11	0.22	0.58	2.17	0.95

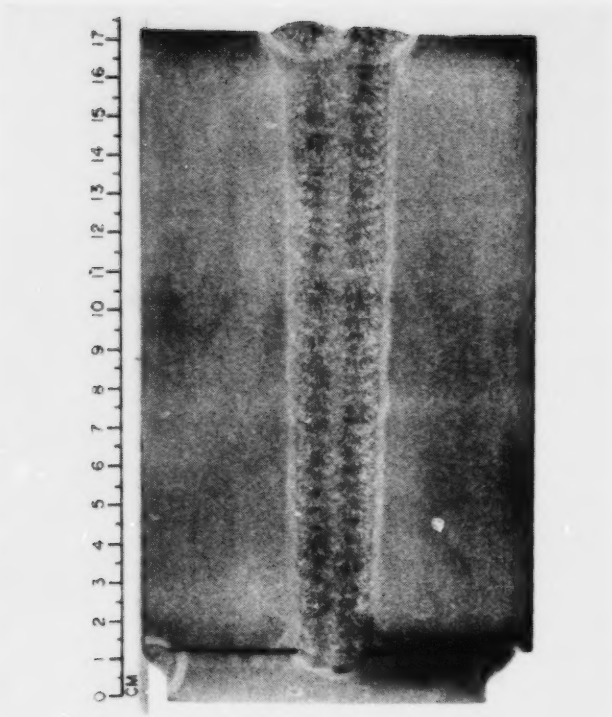

Fig. 7. Macrosection of 150 mm thick section submerged-arc narrow gap weld showing bead shape and overlap configuration. (neg 13930)

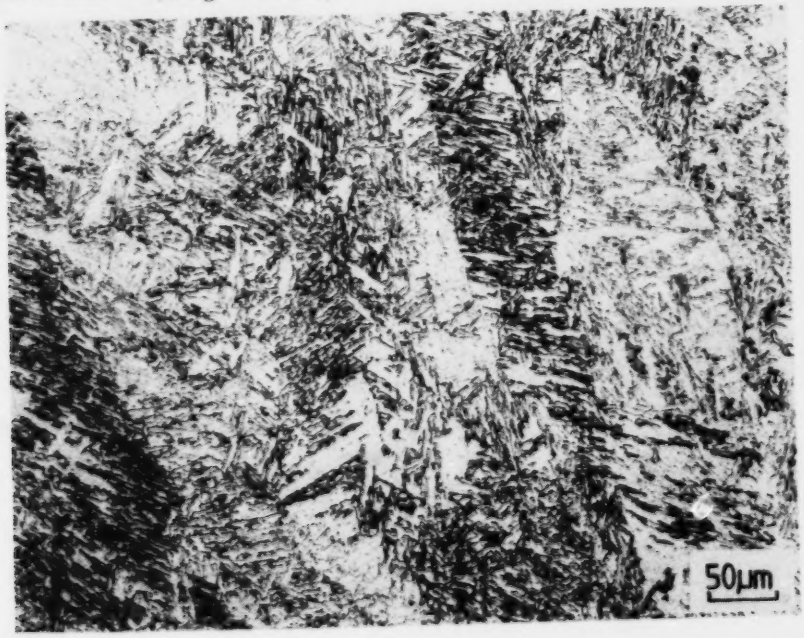

Fig. 8. Representative microstructure of thick section SAW-NG weld. (neg 15369)